

Dual MeV Gamma-Ray and Dark Matter Observatory - GRAMS Project

TSUGUO ARAMAKI,¹ PER HANSSON ADRIAN,¹ CHARLES HAILEY,² GEORGIA KARAGIORGI,² AND HIROKAZU ODAKA³

¹*SLAC National Accelerator Laboratory, Menlo Park, CA 94025, USA*

²*Department of Physics, Columbia University, New York, NY 10027, USA*

³*Department of Physics, University of Tokyo, Tokyo 113-0033, Japan*

ABSTRACT

GRAMS (Gamma-Ray and AntiMatter Survey) is a novel project that is the first to target both astrophysical observations with MeV gamma-rays and an indirect dark matter search with antimatter. The GRAMS instrument is designed with a cost-effective, large-scale LArTPC (Liquid Argon Time Projection Chamber) detector surrounded by plastic scintillators. The astrophysical observations at MeV energies have not yet been well-explored (the so-called 'MeV-gap') and GRAMS can open a new window in this energy region. GRAMS can improve sensitivity by more than an order of magnitude compared to previous experiments. The GRAMS detector is also optimized for cosmic-ray antimatter surveys to indirectly search for dark matter. In particular, low-energy antideuterons will provide an essentially background-free dark matter signature. With an exceptional sensitivity, GRAMS would be able to detect antideuterons from dark matter annihilation or decay even with a single balloon flight. GRAMS would also be able to investigate and validate possible dark matter signatures suggested by the Fermi Gamma-ray Space Telescope and the Alpha Magnetic Spectrometer.

Keywords: MeV gamma-rays, dark matter, antimatter, antiprotons, antideuterons, antiheliums, GRAMS, LArTPC, GAPS, AMS-02, Fermi GCE

1. INTRODUCTION

In recent astrophysical observations, the Large Area Telescope on the Fermi Space Telescope (Fermi-LAT) and the Nuclear Spectroscopic Telescope Array (NuSTAR) opened new windows to survey astrophysical phenomena in the energy domains for hard X-rays (up to 80 keV) and high-energy gamma-rays (above 20 MeV), respectively (Atwood et al. 2009; Harrison et al. 2013). However, gamma-rays in the MeV energy range have not yet been well-explored (the so-called 'MeV gap'). COMPTEL (The Imaging COMPton TELEscope) produced the first catalogue of MeV sources, but only approximately 30 objects have been detected (Schönfelder et al. 2000). Gamma-ray line astronomy, particularly in the MeV energy region, is the key to understanding nucleosynthesis processes by direct observations of nuclear emission lines. The radioactive isotopes can serve as chronometers and tracers while providing information on the physical conditions during nucleosynthesis.

Moreover, energetic particle acceleration can be studied through MeV gamma-ray observations since the transition from thermal to non-thermal physical processes occurs in the MeV energy region. These phenomena can be seen in relativistic flows generated in stellar mass black holes, supermassive black holes in active galactic nuclei and various types of neutron stars such as radio pulsars and magnetars. In addition, multi-messenger astronomy is an important means to understand astrophysical objects including transient phenomena. MeV gamma-rays may be produced in association with gravitational waves from neutron star mergers (Abbott et al. 2017).

Astrophysical observations of gravitational lensing, the Bullet Cluster, and galaxy rotation curves have indicated the existence of dark matter since the 1960s. The nature and origin of dark matter are still unknown, and many theories and experiments have been proposed to understand dark matter. The recent results of Fermi-LAT and Alpha Magnetic Spectrometer (AMS-02) suggested possible dark matter signatures in gamma-ray observations and antiproton measurements respectively (Calore et al. 2015; Daylan et al. 2016; Abazajian & Keeley 2016; Ackermann et al. 2017; Korsmeier et al. 2018). A new approach/experiment is necessary to val-

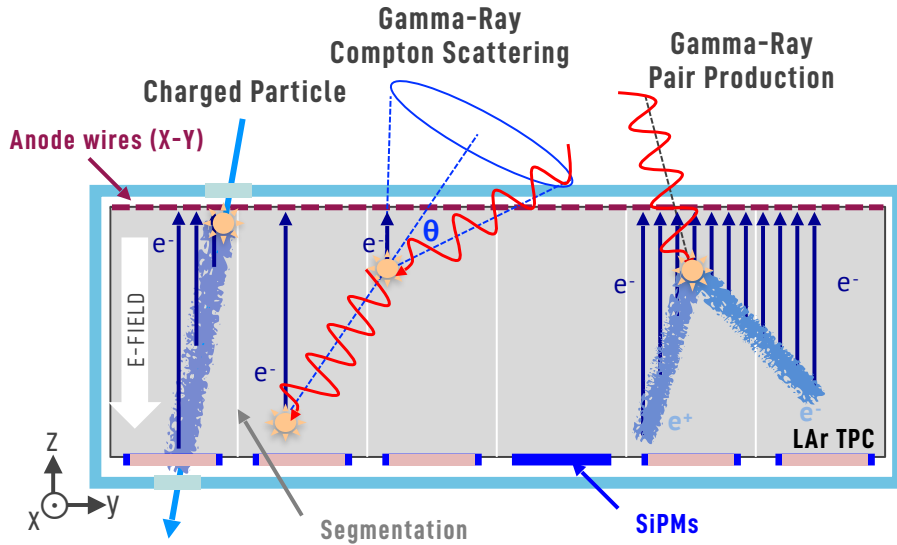


Figure 1. Detection concept for charged particles and gamma-rays (Compton scattering and pair-production).

idate these possible dark matter signatures since astrophysical objects such as millisecond pulsars could mimic the gamma-ray signatures while there are uncertainties in the hadronization and propagation models for the background antiproton production mechanism that may indicate a cosmic-ray origin.

GRAMS (Gamma-Ray and AntiMatter Survey) is a novel project that is the first to target both astrophysical observations with MeV gamma-rays and an indirect dark matter search with antimatter using a Liquid Argon Time Projection Chamber (LArTPC) detector. The LArTPC has been widely used as a large-scale, low-noise detector for neutrino and dark matter search experiments since the 1970s (Rubbia 1977; Cerri & Sergiampietri 1977) and it is directly applicable to a balloon-borne/satellite-based mission. The large-scale LArTPC detector in GRAMS, unlike current and previous experiments with semiconductors or scintillation crystals, can have enhanced sensitivities to gamma-rays and antiparticles as described in the following sections.

2. INSTRUMENT DESIGN

The GRAMS instrumentation is composed of a LArTPC detector surrounded by two layers of plastic scintillators. Unlike semiconductor or scintillation detectors, the GRAMS detector is cost-effective, which allows to have a large-scale detector since argon is both plentiful and cheap. The LArTPC detector works as a Compton camera and a calorimeter for MeV gamma-ray observations as well as a particle tracker for antimatter measurements. The plastic scintillators will veto the incoming charged particles for MeV gamma-ray observations while triggering the incoming particles for

antimatter detection by measuring the time-of-flight (TOF) between the outer and inner scintillator layers (see Figure 2). The LArTPC detector and the readout electronics will be cooled down to ~ 85 Kelvin while the plastic scintillators will be operated at ambient temperature.

Particles entering the LArTPC detector excite and ionize Argon atoms, producing scintillation light and ionization electrons. The scintillation light measured by Silicon Photo-Multipliers (SiPMs) is used for triggering and timing of the event. The ionization electrons drift in an applied electric field and are collected at anode wires oriented in the x and y directions with a ~ 2 mm pitch. The signals induced on the anode wires provide the x and y coordinates of the event, while the drift time of the ionization electrons gives the z position. The ability to reconstruct 3D space points without a multi-layered design is one of the key advantages for GRAMS compared to other gamma-ray detectors with semiconduc-

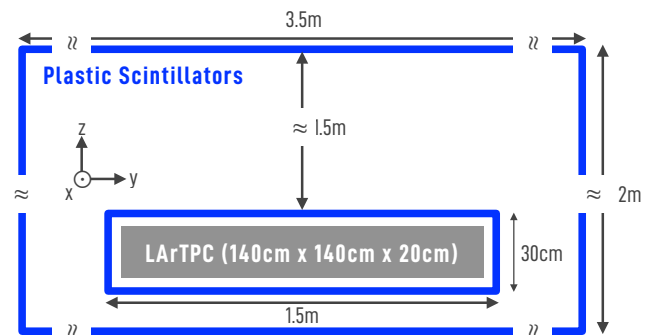


Figure 2. GRAMS detector: LArTPC surrounded by plastic scintillators

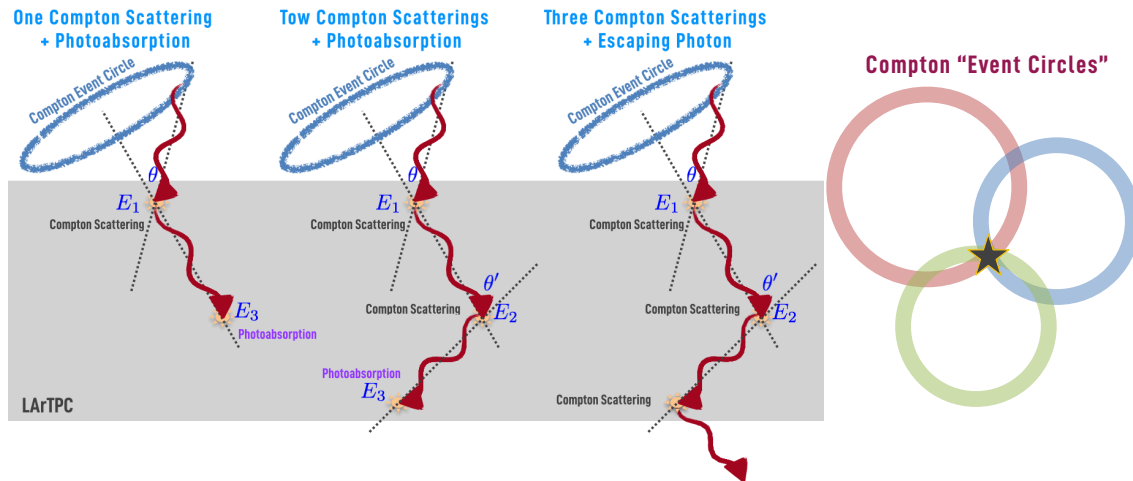


Figure 3. Compton-scattering events in GRAMS. Three or more Compton 'Event Circles' provide the direction of the gamma-ray source.

tors or scintillation crystals. To reduce the coincident background during the finite collection time of the ionization signal, the LArTPC drift volume is segmented into 'cells' with PTFE sheets (see Figure 1). The detector can be further upgraded for a future satellite mission by using a fine pitch (~ 0.2 mm) of anode wires to track Compton-scattered electrons and adding a calorimeter around the detector to measure the escaping gamma-rays and pair-produced electrons and positions.

3. MEV GAMMA-RAY OBSERVATION

3.1. Detection Concept

The MeV gamma-ray survey requires accurate reconstruction of the photon energy and direction. For energies above the electron-positron pair-production threshold ($E > 2m_e c^2$), GRAMS uses the precise tracking capability of the LArTPC to reconstruct the momentum of the electron-positron to determine the incident gamma-ray. At lower energies, where gamma-rays preferably undergo a Compton scattering and a photo-absorption, GRAMS relies on accurately determining the position and energy of the Compton electron and photo-absorption. Reconstruction of the incident gamma-ray energy E and cone angle θ can be estimated by the Compton equation (Kamae et al. 1987; Dogan et al. 1990). A gamma-ray may undergo a number of Compton scatterings before being photo-absorbed or even escape the sensitive volume of the detector (see Figure 3). For one or two Compton scatterings followed by photo-absorption, the energy and cone angle can be calculated as below.

$$E = E_1 + E_2 + E_3$$

$$\cos\theta = 1 - m_e c^2 \left(\frac{1}{E_2 + E_3} - \frac{1}{E_1 + E_2 + E_3} \right)$$

$$\cos\theta' = 1 - m_e c^2 \left(\frac{1}{E_3} - \frac{1}{E_2 + E_3} \right)$$

where m_e is the electron mass, E_1 , E_2 , and E_3 are the deposited energies by the Compton scatterings and photo-absorption, and θ and θ' are the first and the second Compton scattering angles. For a single Compton scattering followed by a photo-absorption, the above simplifies since there is no θ' and $E_2 = 0$. For an event with three or more Compton scatterings, the angle and energy can be reconstructed as below.

$$E = E_1 + E_2 + E'_3$$

$$\cos\theta = 1 - m_e c^2 \left(\frac{1}{E_2 + E'_3} - \frac{1}{E_1 + E_2 + E'_3} \right)$$

$$E'_3 = -\frac{E_2}{2} + \sqrt{\frac{E_2^2}{4} + \frac{E_2 m_e c^2}{1 - \cos\theta'}}$$

where E'_3 is the energy of the gamma-ray just after the second Compton scattering. The gamma-ray after three or more Compton scatterings may escape from the detector. In each case, the cone angle θ gives a Compton 'Event Circle' for each event, and the overlap of three or more 'Event Circles' pinpoints the direction of the gamma-ray source (see Figure 3).

3.2. Effective Area

The effective area for gamma-rays with energy of $0.1 \text{ MeV} < E < 100 \text{ MeV}$ was estimated using a GEANT4

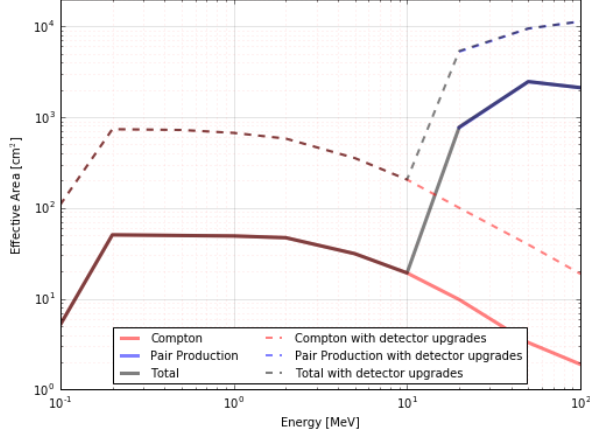


Figure 4. Effective areas for Compton scattering and pair-production events in GRAMS (solid lines). The dashed lines represent the effective areas with detector upgrades.

simulation (Agostinelli et al. 2003). For reliable event reconstruction, events with one or two Compton scatterings followed by photo-absorption or three Compton scatterings inside the LArTPC detector were considered. In order to improve the angular resolution, a set of event selections was also applied; Compton scatterings must be spatially separated by ≥ 10 (2) cm, and pair-produced electrons and positrons must stop inside the sensitive volume and leave tracks ≥ 2 (0.4) cm long (with detector upgrades). Figure 4 shows the effective areas for Compton scattering and pair-production events in GRAMS (solid lines). The dashed lines represent the effective areas with detector upgrades.

3.3. Angular and Energy Resolution

The angular resolution σ_θ for Compton scattering events can be estimated as below (Odaka et al. 2007).

$$\begin{aligned}\sigma_\theta^2 &= \delta\theta_E^2 + \delta\theta_r^2 + \delta\theta_{DB}^2 \\ \delta\theta_E &\simeq \frac{\sigma_E}{E} \\ \delta\theta_r &= \frac{\sigma_r}{d}\end{aligned}$$

where σ_E is the energy resolution at E , σ_r is the spatial resolution of the LArTPC, d is the distance between the Compton scattering(s) and the photo-absorption, and $\delta\theta_{DB}$ is the uncertainty due to the Doppler broadening effect in the Compton scattering (Boggs & Jean 2001; Zoglauer & Kanbach 2003). The energy resolution of LArTPC is estimated from measurements by other experiments deploying similar detectors; DarkSide-50 and

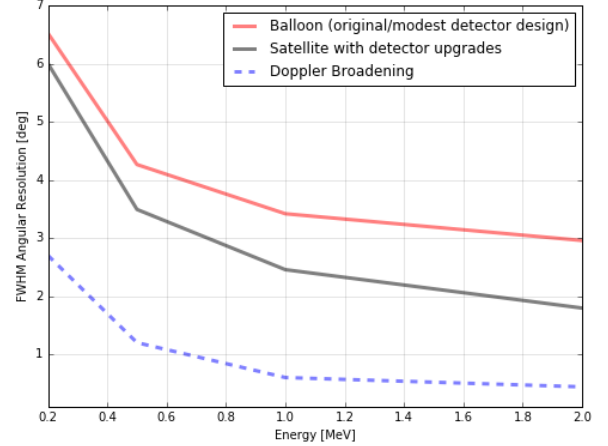


Figure 5. The FWHM angular resolution in GRAMS compared with the uncertainty due to the Doppler broadening effect in the Compton scattering.

nEXO measured $\sigma_E \sim 5\%$ at 41.5 keV and $\sim 1\%$ at 2.5 MeV, respectively (Agnes et al. 2015; Albert et al. 2018).

$$\begin{aligned}\sigma_E^2 &= \Delta E_s^2 + \Delta E_e^2 \\ \frac{\Delta E_s}{E} &\simeq \frac{1\%}{\sqrt{E \text{ (MeV)}/2.5}}\end{aligned}$$

where ΔE_e is the noise contribution from the electronics (~ 5 keV) and ΔE_s is the statistical uncertainty for scintillation light and ionization electrons.

Figure 5 shows the Full Width at Half Maximum (FWHM, $2.35\sigma_\theta$) of the angular resolution in GRAMS compared with the uncertainty due to the Doppler broadening effect in the Compton scattering. The angular resolution could be significantly improved with detector upgrades in the satellite mission, using a fine pitch of anode wires and an additional calorimeter as mentioned above.

3.4. Sensitivity

The gamma-ray continuum sensitivity ($S_{cnt,k}$ [$ph/cm^2/MeV/s$]) in GRAMS was estimated assuming a background count limited observation.

$$S_{cnt,k}(E) \simeq k \sqrt{\frac{\Phi_B \Delta\Omega}{A_{eff} T \Delta E}}$$

where k is the significance level of the source detection, Φ_B [$ph/cm^2/MeV/sr/s$] is the background flux ob-

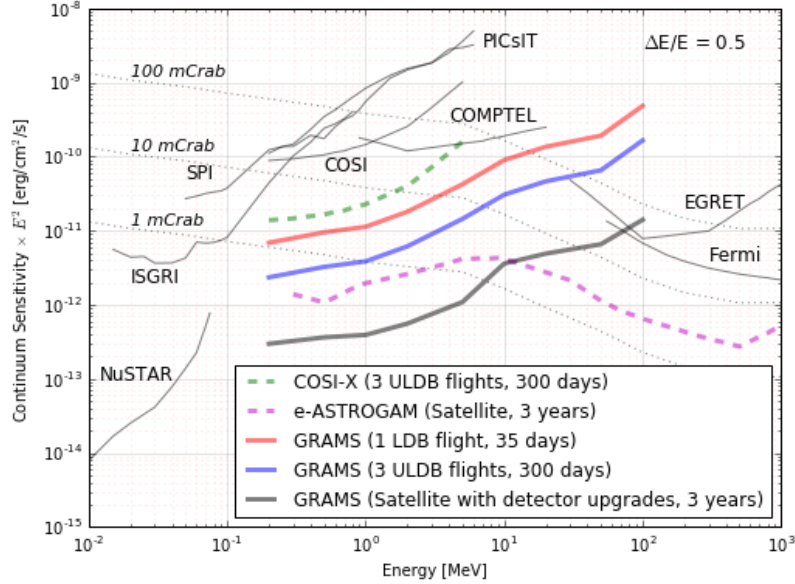


Figure 6. The 3σ continuum sensitivities for GRAMS one LDB flight (35 days), three ULDB flights (300 days) and a future satellite mission with detector upgrades (three year observation time) compared to the ones for previous and future experiments. Black dashed lines represent the flux levels of 1-100 mCrab (Takahashi et al. 2012; De Angelis et al. 2017).

tained from EXPACS¹, T [s] is the observation time, ΔE [MeV] is the energy bandwidth around E ($\Delta E = 0.5E$), and $\Delta\Omega$ [sr] is the solid angle corresponding to the angular resolution.

Figure 6 shows the 3σ continuum sensitivities for one Long-Duration Balloon (LDB) flight (35 days), three Ultra-Long-Duration Balloon (ULDB) flights (3×100 days) and a future satellite mission with detector upgrades (three year observation time). Flux levels for 1-100 mCrab are shown for reference. GRAMS would be able to extensively explore gamma-rays in the MeV energy domain. In particular, the sensitivity for a single LDB flight (35 days) could be an order of magnitude improved sensitivity compared to previous experiments² (Takahashi et al. 2012) and a few times better than the one for the proposed COSI-X mission³ with three ULDB flights (3×100 days). The sensitivity for the GRAMS three ULDB flights could further improve the sensitiv-

ity by a factor of 3 and the sensitivity for the GRAMS satellite mission could be a few times better than the one for e-ASTROGAM at $E < 10$ MeV. e-ASTROGAM is a future satellite mission that requires ~ 50 layers of double-sided silicon strip detectors with a large number ($\sim 10^6$) of channels/electronics (De Angelis et al. 2017) while GRAMS uses a cost-effective LArTPC detector with a smaller number ($\sim 10^4$ with a fine pitch of anode wires) of channels/electronics.

Sensitivity [ph/cm ² /s]	GRAMS	SPI/INTEGRAL	Improvement Factor
e^+ (511 keV)	1.3×10^{-6}	5.0×10^{-5}	~ 40
^{56}Co (847 keV)	7.5×10^{-7}	$\sim 2 \times 10^{-5}$	~ 25
^{44}Ti (1157 keV)	6.3×10^{-7}	$\sim 2 \times 10^{-5}$	~ 30
^{60}Fe (1173 keV)	6.3×10^{-7}	$\sim 2 \times 10^{-5}$	~ 30
^{22}Na (1275 keV)	6.1×10^{-7}	$\sim 2 \times 10^{-5}$	~ 30
^{60}Fe (1333 keV)	5.9×10^{-7}	$\sim 2 \times 10^{-5}$	~ 30
^{26}Al (1809 keV)	5.2×10^{-7}	2.5×10^{-5}	~ 50
^2H (2223 keV)	4.8×10^{-7}	$\sim 2 \times 10^{-5}$	~ 40
$^{12}\text{C}^*$ (4438 keV)	4.0×10^{-7}	$\sim 1 \times 10^{-5}$	~ 25

Table 1. The GRAMS line sensitivity to positron annihilation and radioactive isotopes compared with SPI/INTEGRAL (3σ , observation time = 10^6 s).

¹ EXcel-based Program for calculating Atmospheric Cosmic-ray Spectrum (EXPACS) instantaneously calculates terrestrial cosmic ray fluxes of neutrons, protons, and ions with charge up to 28 (Ni) as well as muons, electrons, positrons, and photons nearly anytime and anywhere in the Earth's atmosphere (<https://phits.jaea.go.jp/expacs/>).

² COSI collaboration website (The Compton Spectrometer and Imager, <http://cosi.ssl.berkeley.edu>)

³ The sensitivity was estimated based on the observation time and improved angular resolution, compared to the COSI sensitivity.

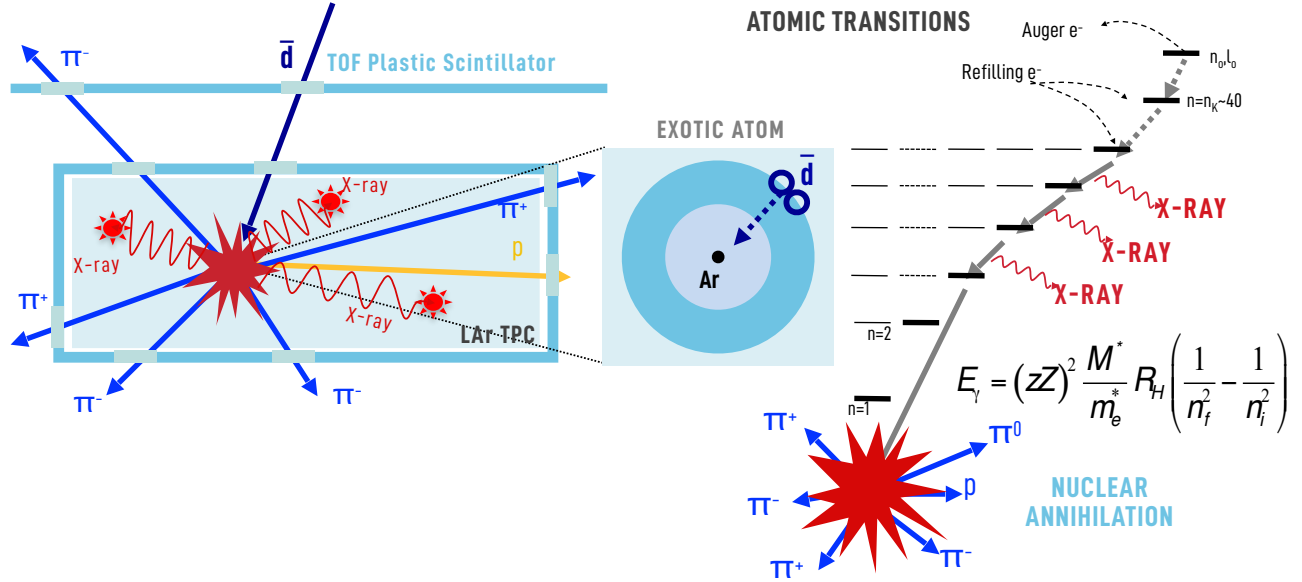


Figure 7. The GRAMS antimatter detection technique. The stopped antimatter forms an excited exotic atom that decays and emits atomic X-rays and annihilation products (pions and protons). The atomic X-rays, pion/proton multiplicities, and the stopping depth in the LArTPC provide the particle identification capability.

The sensitivity to gamma-ray lines from positron annihilation and radioactive isotopes ($S_{line,k}$ [$ph/cm^2/s$]) was also estimated. The bandwidth (ΔE) was chosen as $2\sigma_E$ at each energy.

$$S_{line,k}(E) \simeq k \sqrt{\frac{\Phi_B \Delta \Omega \Delta E}{A_{eff} T}}$$

Table 1 shows the sensitivity (3σ , observation time $T = 10^6$ s) to gamma-ray lines from positron annihilation (511 keV), ^{56}Co (847 keV) from thermonuclear supernovae, ^{44}Ti (1157 keV) from core-collapse supernovae, ^{22}Na (1275 keV) from classical novae, ^{60}Fe (1173 keV and 1333 keV) from core-collapse supernovae, ^{26}Al (1809 keV) from collapse supernovae or massive stars, ^2H (2223 keV) from neutron capture by protons, and $^{12}\text{C}^*$ (4438 keV) from cosmic-ray interactions (Knödlseher & Vedrenne 2001; Diehl 2013). With this larger effective area, GRAMS would have an order of magnitude improved sensitivity compared with SPI/INTEGRAL (Jean et al. 2000; Roques et al. 2003).

4. ANTIMATTER SURVEY

4.1. Detection Concept

The GRAMS antimatter survey involves capturing an antiparticle in a target material with subsequent formation and decay of an exotic atom, similar to the GAPS project (Mori et al. 2002; Aramaki et al. 2013, 2016). The TOF plastic scintillators measure the ve-

locity and angle of the incoming antiparticle. The antiparticle slows down and stops inside the LArTPC detector, where it forms an excited exotic atom with an Argon atom. Then, the exotic atom emits atomic X-rays as it de-excites. The energy of the atomic X-ray depends on the mass and atomic number of the antiparticle and the target atom. The two highest atomic X-rays for an exotic atom with an antiproton and an Argon atom are 58 keV and 97 keV, and 74 keV and 114

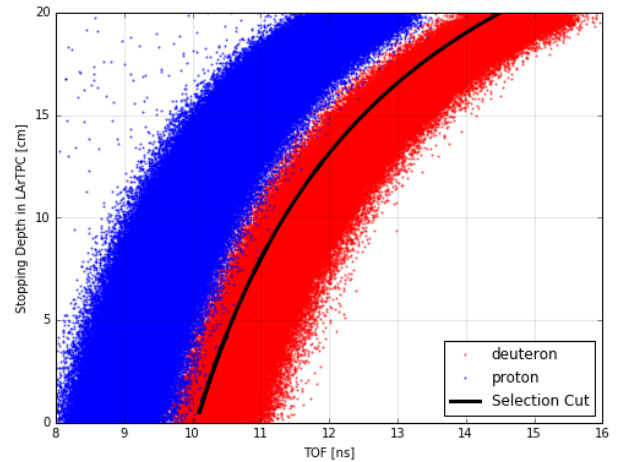


Figure 8. The simulation result for the stopping range of (anti)protons and (anti)deuterons taking into account the position resolution of ~ 3 mm in the LArTPC detector and the timing resolution of ~ 0.4 ns in the TOF system. The solid black line represents the selection cut.

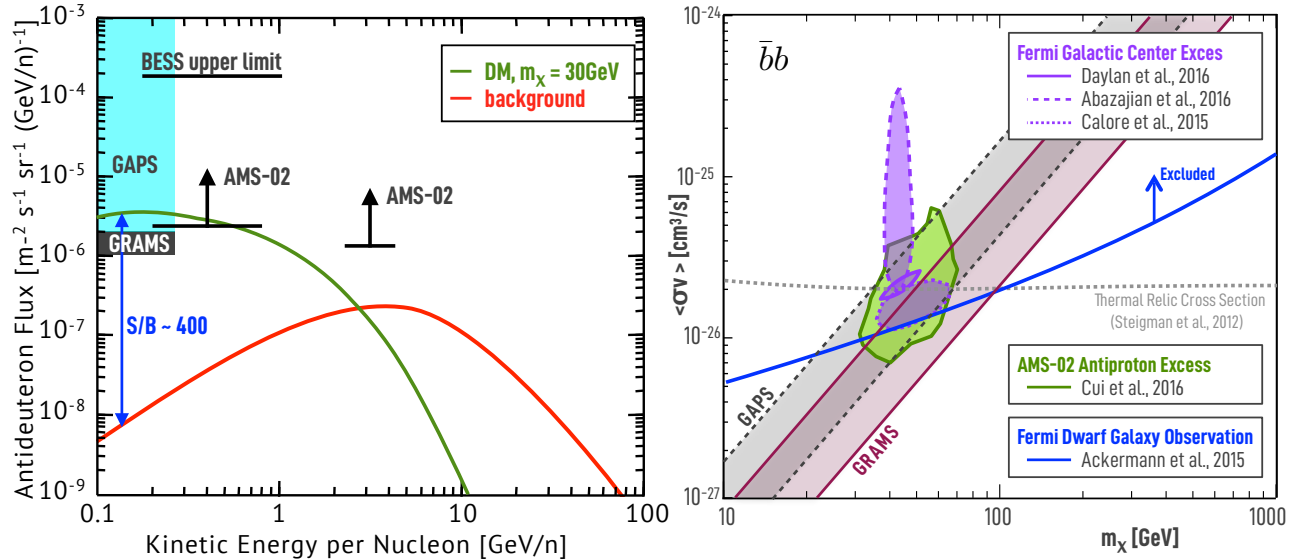


Figure 9. The left figure shows the antideuteron sensitivities for GRAMS (three LDB flights from Antarctica, 105 days) and other experiments together with the predicted antideuteron fluxes from dark matter annihilation (primary) and cosmic-ray interactions (secondary) (Donato et al. 2000; Fuke et al. 2005; Aramaki et al. 2016; Ong et al. 2017; Donato et al. 2008; Ibarra & Wild 2013). The right figure shows the parameter space for the possible dark matter signatures suggested by Fermi and AMS-02 (Calore et al. 2015; Daylan et al. 2016; Abazajian & Keeley 2016; Ackermann et al. 2017; Korsmeier et al. 2018), where GRAMS and GAPS sensitivities are overlaid with an uncertainty of the antideuteron production model (Fornengo et al. 2013; Acharya et al. 2018; Korsmeier et al. 2018).

keV with an antideuteron and an Argon atom. At the end of the atomic cascade, the antiparticle subsequently annihilates in the nucleus with the emission of pions and protons. The number of pions and protons produced (pion/proton multiplicity) is roughly proportional to the number of antinucleons in the incoming antiparticle. This pion/proton multiplicity can also be used to identify the incoming antiparticle. The detection concept was validated in detail with antiproton beam tests at the KEK accelerator, where the X-ray yields from exotic atoms of different target materials were measured (Hailey et al. 2006; Aramaki et al. 2013).

Additionally, GRAMS can measure the stopping range of the incoming antiparticles with an excellent position resolution in the LArTPC. Figure 8 shows the simulation results for the stopping range study, assuming the position resolution of ~ 3 mm in the LArTPC detector and the timing resolution of ~ 0.4 ns in the TOF system. Here, protons and deuterons were used instead of antiprotons and antideuterons to simplify the physics process. The solid black line represents the selection cut while the acceptances (probabilities for events in the right side of the selection cut) are 2.7×10^{-6} for antiprotons and 0.74 for antideuterons. These particle identification techniques (atomic X-rays, pion/proton multiplicities, and stopping range) will allow us to distinguish incoming antideuterons from others and the expected

mimic/background events could be as small as 0.01 during the LDB flight.

4.2. Sensitivity

The left panel of Figure 9 shows the GRAMS antideuteron sensitivity (three LDB flights from Antarctica, 105 days) together with the predicted antideuteron fluxes from dark matter annihilation (primary) and cosmic-ray interactions (secondary/background). The primary antideuteron flux can be more than two orders of magnitude larger than the secondary flux at low-energy (Donato et al. 2000, 2008; Ibarra & Wild 2013). Therefore, the GRAMS antideuteron measurement is essentially a background-free dark matter search and provides stringent constraints on a variety of dark matter models. The GRAMS antideuteron sensitivity could be a few times better than GAPS (three LDB flights, 105 days) and AMS-02⁴ (five years of observation), and more than two orders of magnitude better than the current upper limit obtained by BESS (Fuke et al. 2005; Aramaki et al. 2016; Ong et al. 2017). With this improved sensitivity, GRAMS would be able to detect antideuterons from the dark matter annihilation or

⁴ The AMS-02 sensitivity is a strict upper limit since it is based on the superconducting magnet, rather than the permanent magnet used in the actual flight.

decay with a single balloon flight, unlike other experiments.

The recent results of the Fermi gamma-ray observation from the Galactic Center region and spheroidal dwarf galaxies as well as the AMS-02 antiparticle measurements indicate the detection of possible dark matter signatures (Calore et al. 2015; Daylan et al. 2016; Abazajian & Keeley 2016; Ackermann et al. 2017; Korsmeier et al. 2018). This is, however, not conclusive and a new approach/experiment like GRAMS is essential to validate these results. The right panel of Figure 7 shows the parameter space for the possible dark matter signatures suggested by Fermi and AMS-02, where GRAMS and GAPS sensitivities are overlaid with an uncertainty of the antideuteron production model (Fornengo et al. 2013; Acharya et al. 2018; Korsmeier et al. 2018). GRAMS would be able to fully investigate and could substantiate these results. Furthermore, GRAMS could investigate the low-energy antiprotons for dark matter signatures as well as the possible antideuteron/antihelium detections suggested by AMS-02 with a complementary detection technique, which is crucial to validate rare event defections (Aramaki et al. 2014; Korsmeier et al. 2018). The GRAMS detector is relatively simple to configure and we can expect to have multiple balloon flights per a few years with a smooth detector recovery, which will allow us to further improve

the sensitivities for both MeV gamma-ray and antimatter measurements.

5. CONCLUSION

GRAMS is the first balloon experiment optimized for both MeV gamma-ray observations and an indirect dark matter search with a LArTPC detector. GRAMS can open a new window in the MeV energy domain for astrophysical observations while simultaneously investigating dark matter parameter space with antimatter measurements. With a cost-effective, large-scale LArTPC detector, a single LDB flight can have more than an order of magnitude improved sensitivity for MeV gamma-ray observation compared to the previous experiments. With an excellent particle identification capability, GRAMS sensitivity to antideuterons could be a few times better compared to the previous/proposed experiments, which may allow us to detect antideuterons as a dark matter signature even with a single balloon flight.

6. ACKNOWLEDGMENTS

This work is supported and funded by Department of Energy (DE-AC02-76SF00515) and NASA APRA Grants (NNX09AC16G). We would like to thank Tom Shutt, Kazuhiro Terao, Greg Madejski, and Chris Stanford at SLAC/Stanford University as well as Yoshiyuki Inoue at RIKEN for helpful discussions.

REFERENCES

- Abazajian, K. N., & Keeley, R. E. 2016, *Physical Review D*, 93, 083514
- Abbott, B., Abbott, R., Adhikari, R., et al. 2017, *Astrophysical Journal Letters*, 848, L12
- Acharya, S., Adam, J., Adamová, D., et al. 2018, *Physical Review C*, 97, 024615
- Ackermann, M., Ajello, M., Albert, A., et al. 2017, *The Astrophysical Journal*, 840, 43
- Agnes, P., Alexander, T., Alton, A., et al. 2015, *Physics Letters B*, 743, 456
- Agostinelli, S., Allison, J., Amako, K. a., et al. 2003, *Nuclear instruments and methods in physics research section A: Accelerators, Spectrometers, Detectors and Associated Equipment*, 506, 250
- Albert, J., Anton, G., Arnquist, I., et al. 2018, *Physical Review C*, 97, 065503
- Aramaki, T., Chan, S., Craig, W., et al. 2013, *Astroparticle Physics*, 49, 52
- Aramaki, T., Boggs, S., von Doetinchem, P., et al. 2014, *Astroparticle Physics*, 59, 12
- Aramaki, T., Hailey, C., Boggs, S., et al. 2016, *Astroparticle Physics*, 74, 6
- Atwood, W., Abdo, A. A., Ackermann, M., et al. 2009, *The Astrophysical Journal*, 697, 1071
- Boggs, S., & Jean, P. 2001, *Astronomy & Astrophysics*, 376, 1126
- Calore, F., Cholis, I., McCabe, C., & Weniger, C. 2015, *Physical Review D*, 91, 063003
- Cerri, C., & Sergiampietri, F. 1977, *Nuclear Instruments and Methods*, 141, 207
- Daylan, T., Finkbeiner, D. P., Hooper, D., et al. 2016, *Physics of the Dark Universe*, 12, 1
- De Angelis, A., Tatischeff, V., Tavani, M., et al. 2017, *Experimental Astronomy*, 44, 25
- Diehl, R. 2013, *The Astronomical Review*, 8, 19
- Dogan, N., Wehe, D. K., & Knoll, G. F. 1990, *Nuclear Instruments and Methods in Physics Research Section A: Accelerators, Spectrometers, Detectors and Associated Equipment*, 299, 501
- Donato, F., Fornengo, N., & Maurin, D. 2008, *Physical Review D*, 78, 043506

- Donato, F., Fornengo, N., & Salati, P. 2000, *Physical Review D*, 62, 43003
- Fornengo, N., Maccione, L., & Vittino, A. 2013, *Journal of Cosmology and Astroparticle Physics*, 2013, 031
- Fuke, H., Maeno, T., Abe, K., et al. 2005, *Physical review letters*, 95, 081101
- Hailey, C., et al. 2006, *Astropart. Phys. JCAP01*, 7
- Harrison, F. A., Craig, W. W., Christensen, F. E., et al. 2013, *The Astrophysical Journal*, 770, 103
- Ibarra, A., & Wild, S. 2013, *Physical Review D*, 88, 023014
- Jean, P., Vedrenne, G., Schönfelder, V., et al. 2000, *AIP Conference Proceedings*, 510, 708
- Kamae, T., Enomoto, R., & Hanada, N. 1987, *Nuclear Instruments and Methods in Physics Research Section A: Accelerators, Spectrometers, Detectors and Associated Equipment*, 260, 254
- Knödlseher, J., & Vedrenne, G. 2001, in *Exploring the Gamma-Ray Universe*, Vol. 459, 23–35
- Korsmeier, M., Donato, F., & Fornengo, N. 2018, *Physical Review D*, 97, 103011
- Mori, K., Hailey, C. J., Baltz, E. A., et al. 2002, *The Astrophysical Journal*, 566, 604
- Odaka, H., Takeda, S., Watanabe, S., et al. 2007, *Nuclear Instruments and Methods in Physics Research Section A: Accelerators, Spectrometers, Detectors and Associated Equipment*, 579, 878
- Ong, R., Aramaki, T., Bird, R., et al. 2017, *POS PROCEEDINGS OF SCIENCE*, 1
- Roques, J., Schanne, S., Von Kienlin, A., et al. 2003, *Astronomy & Astrophysics*, 411, L91
- Rubbia, C. 1977, *CERN-EP-INT-77-08*
- Schönfelder, V., Bennett, K., Blom, J., et al. 2000, *Astronomy and Astrophysics Supplement Series*, 143, 145
- Takahashi, T., Stawarz, L., & Uchiyama, Y. 2012, *Astroparticle Physics*, 43, 142
- Zoglauer, A., & Kanbach, G. 2003, in *X-Ray and Gamma-Ray Telescopes and Instruments for Astronomy*, Vol. 4851, *International Society for Optics and Photonics*, 1302–1310